Springer

KSME

Journal of Mechanical Science and Technology 29 (8) (2015) 3153~3163
www.springerlink.com/content/1738-494x(Print)/1976-3824(Online)
DOI 10.1007/s12206-015-0714-9

Code-to-code comparison study on rotor aeromechanics in descending flight †

Jae-Sang Park[1,*] and Young Jung Kee[2]

[1]*Department of Aerospace Engineering, Chungnam National University, 99 Daehak-ro, Yuseong-gu, Daejeon, 305-764, Korea*
[2]*Rotorcraft Research Team, Korea Aerospace Research Institute, 169-84 Gwahak-ro, Yuseong-gu, Daejeon, 305-806, Korea*

(Manuscript Received November 10, 2014; Revised March 11, 2015; Accepted March 17, 2015)

Abstract

This paper conducts the aeromechanics study using the two different rotorcraft computational structural dynamics (CSD) codes, CAMRAD II and DYMORE II, for the rotor in low-speed descending flight. The three test cases of the HART (Higher-harmonic control aeroacoustic rotor test) I -baseline, minimum noise, and minimum vibration- are considered in this study of the blade-vortex interaction (BVI) airloads, rotor trim, blade elastic deformations, and blade structural loads. The two prediction results are compared to each other for a code-to-code comparison study as well as to the measured data. Although CAMRAD II and DYMORE II use different theories and models, most of the prediction results are similar to each other and compared fairly well with the wind tunnel test data. For all the three test cases, the two rotorcraft CSD analyses show good prediction on the fluctuations of the section normal force (M^2C_n) due to BVI, but both over-predict the trimmed collective pitch angle. The blade elastic deformations, such as flap deflection and elastic torsion deformation at the tip, are reasonably predicted by both rotorcraft CSD analyses. But, the CAMRAD II result using the multiple-trailer wake model with consolidation is slightly better than the DYMORE II prediction with the single wake panel model particularly for the elastic torsion deformation in the baseline case. In addition, CAMRAD II and DYMORE II both correlate reasonably the blade structural loads, such as flap bending, lead-lag bending, and torsion moments, with the measured data; however, the CAMRAD II results are moderately better than the DYMORE II predictions.

Keywords: Blade-vortex interaction; Comprehensive rotorcraft analysis codes; Rotor aeromechanics; HART

1. Introduction

The blade-vortex interaction (BVI) is caused by interaction between rotor blades and their trailed vortices. This BVI phenomenon occurs mainly in descending flight and low speed transition flight, and it causes significant noise and/or vibration problems. To improve basic understanding of the formation of vortex wakes and their interaction leading to noise and vibration, the international cooperative programs HART (Higher-harmonic control aeroacoustic rotor test) I and II were conducted in 1994 [1] and 2001 [2], respectively. Through these wind tunnel tests, massive measurement data [1, 3] was obtained regarding noise level, blade airloads, vortex wakes, blade elastic deformations, and structural loads, with and without higher harmonic pitch control (HHC) inputs.

Since HART II provides more sophisticated measurements of vortex wakes using an improved technique (3C-PIV: Particle image velocimetry) over wake measurements in HART I, the measured data from HART II have been widely used to validate the comprehensive rotorcraft analyses based on the rotorcraft computational structural dynamics (CSD, [4-7]), computational fluid dynamics (CFD, [8, 9]), and CSD/CFD coupled analyses [10, 11] rather than the wind tunnel test data from HART I. Although HART I was conducted earlier than HART II, the HART I also provides meaningful test data of the rotor aeromechanics, wakes, and acoustics with and without HHC inputs. Above all, the blade airloads in HART I were measured at three blade span locations (75, 87 and 97% span), which is a distinct advantage over HART II which only measured the blade airloads at a single blade span (87% span).

Though correlation works between the rotorcraft CSD analysis and the wind tunnel test data from HART I were conducted by the German DLR, French ONERA, US NASA Langley, and US Army (AFDD) which were the HART I participants through the HART I workshops, there has been limited research [12-18] in public domain as compared to the volume of correlation studies for HART II. Furthermore, most previous works, except Refs. [17, 18], have mainly dealt with the correlation of blade airloads and vortex wake positions with the measured data but have not correlated blade structural loads. Moreover, code-to-code comparison studies using two or more rotorcraft CSD codes on the rotor aeromechanics, except Ref. [12], have not been conducted for HART I, al-

*Corresponding author. Tel.: +82 42 821 6682, Fax.: +82 42 825 9225
E-mail address: aerotor@cnu.ac.kr
† Recommended by Associate Editor Cheolung Cheong

though extensive code-to-code comparison studies [6, 10] using the rotorcraft CSD analyses and the CSD/CFD coupled analyses were recently performed for HART II.

The state-of-the-art rotorcraft CSD codes use different theories and models to analyze the rotor aeromechanics. Therefore, the prediction results by different rotorcraft CSD codes may be different from or similar to each other. The differences and similarities between the results from two or more rotorcraft CSD analyses may suggest a more appropriate theory or model to improve the rotor aeromechanics prediction. Therefore, the present work aims to compare the aeromechanics analyses using the two different rotorcraft CSD codes, CAMRAD (Comprehensive analytical model of rotorcraft aerodynamics and dynamics) II [19] and DYMORE II [20], for HART I with and without HHC inputs. CAMRAD II is a well-known comprehensive rotorcraft analysis code, and DYMORE II is a nonlinear flexible multibody dynamics analysis code that has been used widely for various analyses of rotorcrafts. In this code-to-code comparison study for HART I, the blade section normal forces (M^2C_n), rotor trimmed pitch control angles, blade elastic deformations at the tip, and blade structural loads predicted by both CAMRAD II and DYMORE II are investigated. The two prediction results are compared to each other for the present code-to-code comparison study as well as to the wind tunnel test data.

2. Description of the HART I test

The HART I rotor is a 40% Mach-scaled rotor of the BO-105 main rotor, and it was designed to match the rotating frequencies of the first few modes of the full-scale rotor blade at the nominal rotor speed. An NACA23012 airfoil with a tab was used. The general properties [1] of the HART I rotor blade are summarized in Table 1. In addition, the measured section properties of the uninstrumented blade for the HART I can be found in Ref. [18]. The HART I rotor was tilted by about 5.3° aft in the DNW test, and it had a thrust level (C_T) of 0.0044 at an advance ratio μ of 0.15. For the isolated rotor model in the present study, the fuselage effect as well as the wind tunnel wall effect is considered; thus, the corrected shaft tilting angle of 4.5° is used [18]. The three-per-rev (3P) pitch control inputs given in Table 2 were introduced for the minimum noise (MN) and minimum vibration (MV) cases. These HHC input conditions are slightly different from those for HART II. The pressure on the reference blade (Blade No. 1) surface was measured at three blade stations (75, 87 and 97% span locations) using pressure transducers. The 44, 24 and 44 pressure transducers were distributed in the chordwise direction at 75, 87 and 97% blade stations, respectively. In addition, the reference blade had 32 strain gauges at 16 blade stations between 14 and 83% span to measure the blade elastic deformations and structural loads. Also, the blade motions were verified alternatively by the projected grid method (PGM) and the target attitude in real time method (TART). All the measured data for the present study can be obtained from Ref. [1].

Table 1. General properties of the HART I rotor.

Rotor type	Hingeless
Number of blades, N	4
Rotor radius, R	2.0 m
Location of feathering hinge	0.0375R
Chord length, c	0.121 m
Solidity, σ	0.077
Airfoil section	NACA23012 mod
Blade built-in twist	-8.0° (Linear)
Precone angle	2.5°
Nominal rotor speed, Ω_{ref}	109.0 rad/s

Table 2. Higher harmonic pitch control inputs for the MN and MV cases.

Cases	θ_{3P}	ψ_{3P}
MN	0.87°	296°
MV	0.83°	178°

3. Prediction methods

3.1 Comprehensive rotorcraft analysis: CAMRAD II

CAMRAD II is an analysis of rotorcraft aeromechanics which includes multibody dynamics, nonlinear finite elements, and rotorcraft aerodynamics. Finite nonlinear beam elements with small strain and moderate deflections are used to represent the structural dynamics model of rotor blades. Each beam element has fifteen degrees of freedom which consists of four flap, four lead-lag, three torsion, and four axial variables. The modified ONERA-EDLIN (Equations differentielles linearies) theory is used for the unsteady aerodynamics on the rotor blade. The blade section aerodynamic forces and moments are calculated using the local angle of attack, Mach number at the 3c/4 point, and the aerodynamic coefficients from the C81 airfoil table look-up. The freewake model is essential for the rotorcraft CSD code to predict well the behavior of BVI airloads. Currently CAMRAD II has three freewake models - rolled-up wake, multiple-trailer wake, and multiple-trailer wake with consolidation-. Among these three freewake models, the multiple-trailer wake model with consolidation can give reasonably good results on the rotor aeromechanics prediction [15-17]. In this modeling, the trailed vortex filaments at the aerodynamic panel edges can be consolidated into a single rolled-up filament by the process of entrainment or compression. The Newton-Rapson method is used to obtain the trim solution with the harmonic balance time integration method. Through the trim analysis, the trim variables such as the collective pitch angle, the lateral and longitudinal cyclic pitch angles are determined to satisfy the trim targets.

In the present CAMRAD II modeling for the HART I rotor system, each blade is discretized into 16 nonlinear beam finite elements. Smaller beam elements are used in the inboard of

the rotor blade in order to consider more effectively non-uniform blade structural properties. A torsional spring with a value of 1706 Nm/rad. [18] is used at the feathering hinge to match the measured first torsional frequency (T1) at non-rotating condition [1]. A total of 16 aerodynamic panels [4] are used in the present aerodynamic modeling. The multiple-trailer wake model with consolidation is adopted for the blade vortex wake modeling and the consolidation by compression process is used. Although the single wake panel can be also used in the CAMRAD II modeling for the equivalent condition to the DYMORE II modeling described in the next section, the multiple wake panels are used for the best prediction using more sophisticated wake modeling. The vortex core growth model based on the square root of an azimuthal wake age is used. The trim analysis is performed using a low azimuthal resolution of 15°. However, after trim solution is obtained, the post-trim method using a high azimuthal resolution of 2° is applied to represent reasonably well the fluctuations of the section normal forces due to BVI.

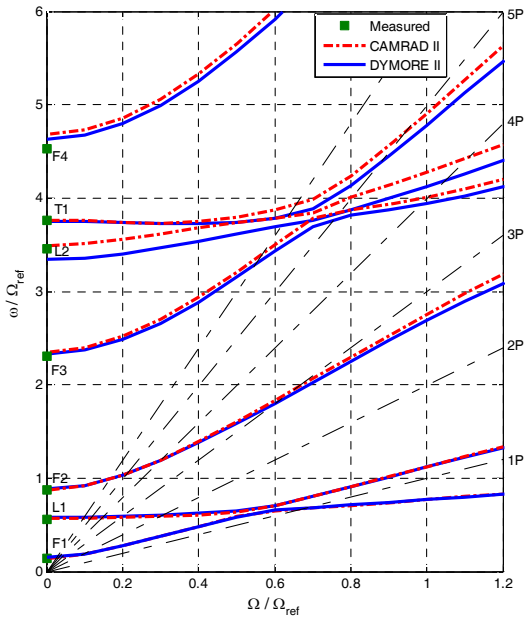

Fig. 1. Correlation of the fan plot analyses.

3.2 Nonlinear flexible multibody dynamics: DYMORE II

The nonlinear flexible multibody dynamics, DYMORE II, is also used as a rotorcraft CSD code for the present code-to-code comparison study. DYMORE II has various multibody elements: rigid bodies, rigid and elastic joints, and nonlinear elastic bodies, such as beams and shells based on the finite element method. The geometrically exact beam theory [21] is used for nonlinear elastic beam modeling. Furthermore, DYMORE II has simple aerodynamic models based on the lifting line theory for rotors and wings. The aerodynamic loads at the airstations located on the lifting line are calculated using the two-dimensional unsteady airfoil theory [22] with the C81 airfoil table look-up. As a rotor inflow model, the finite-state dynamic inflow model [23] is included originally in DYMORE II. However, this inflow model is not appropriate to capture the fluctuation of blade airloads due to BVI [5-7]. Therefore, a general freewake model [24] which was implemented integrally into DYMORE II [5] is used for this work. Squires' square root law [25] is used for the vortex core growth. The autopilot theory [26] is used to adjust the collective, lateral, and longitudinal cyclic pitch control angles to match the trim conditions in wind tunnel test.

In the present DYMORE II modeling for the HART I rotor system, four nonlinear elastic blades and a rigid hub are considered. For the finite element modeling of the blades, each blade is discretized into 15 cubic beam elements. The equivalent torsional spring at the feathering hinge is used to represent the stiffness of the rotor control system. The same value of the torsional spring constant in the CAMRAD II modeling for the HART I rotor system is used. The hub is modeled as a rigid body and connected to a revolute joint with a prescribed rotational speed. For the aerodynamic loads on the blade, 31 airstations are used on each blade. In the freewake modeling, a single wake panel which has two trailed vortex filaments at the blade root-cutout and tip is used. The present DYMORE II analysis is conducted with a high azimuthal resolution of 1°.

4. Results and discussion

4.1 Natural frequencies

Fig. 1 compares the fan plot analyses using CAMRAD II and DYMORE II for the HART I rotor blade with the collective pitch angle of 0°. As seen in the figure, the two prediction results are very close to each other although the second lead-lag frequency (L2) at non-rotating condition by DYMORE II is slightly under-predicted as compared with both the measured data [1] and the present CAMRAD II analysis. Both predictions for the fourth flap frequency (F4) at non-rotating condition are slightly higher than the measured data. Therefore, through this fan plot analysis, it is considered that the two different rotor structural dynamics models have similar characteristics.

4.2 Blade section normal forces

Figs. 2-4 show the correlations of the section normal force, M^2C_n, at r/R = 0.75, 0.87, and 0.97 between the two predictions and the measured data for the BL, MN, and MV cases of HART I. In this work, the comparisons of section pitching moment is not studied since the lifting line theories used in CAMRAD II and DYMORE II do not have BVI-related moment formulation [6]. For the BL case as given in Fig. 2, the measured data at all the three blade span locations show severe fluctuations of section normal forces due to BVI on both advancing and retreating sides. The CAMRAD II and DYMORE II analyses both predict the M^2C_n fluctuations reasonably well, although some of the fluctuations are not pre-

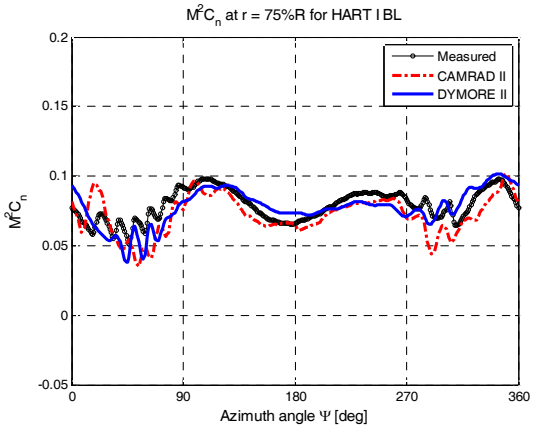

(a) r/R = 0.75

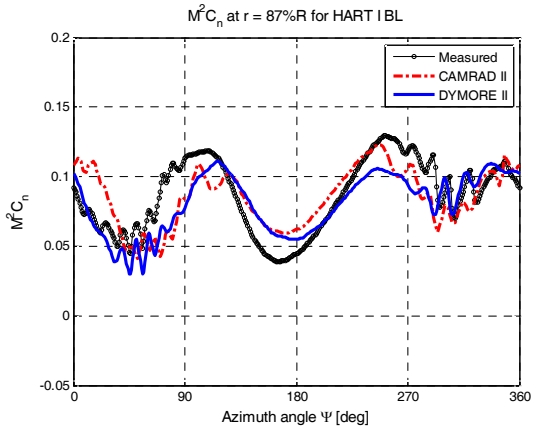

(b) r/R = 0.87

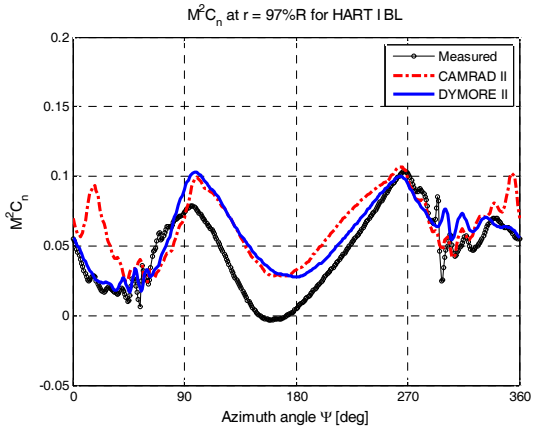

(c) r/R = 0.97

Fig. 2. Correlations of the section normal force (M^2C_n) for the BL case.

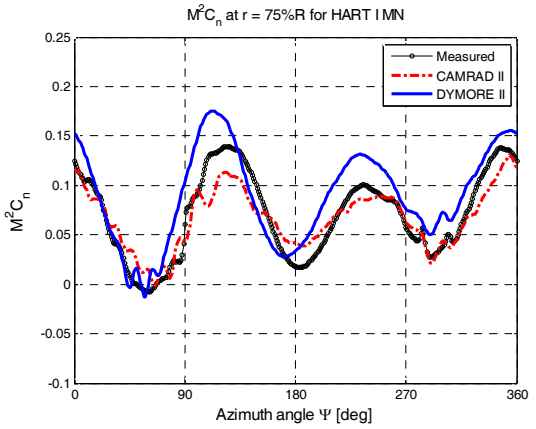

(a) r/R = 0.75

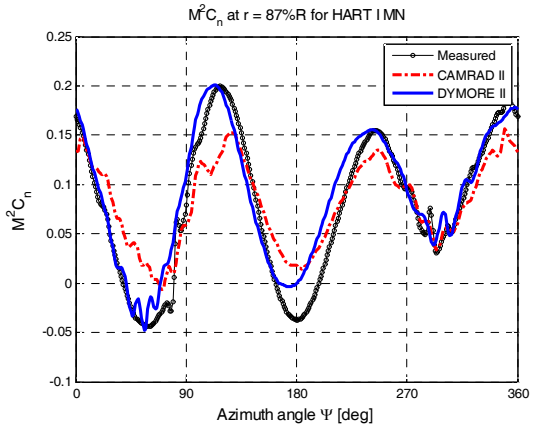

(b) r/R = 0.87

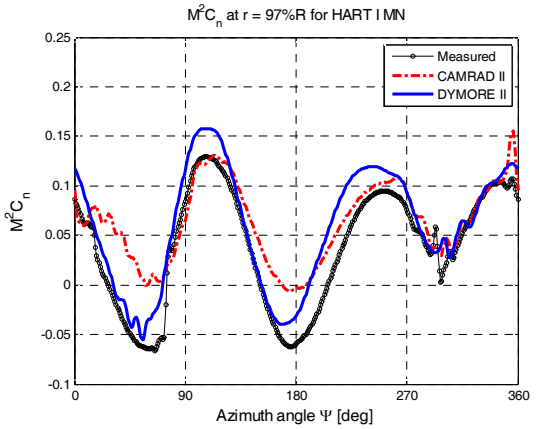

(c) r/R = 0.97

Fig. 3. Correlations of the section normal force (M^2C_n) for the MN case.

dicted, or spurious BVI events are shown. Furthermore the two rotorcraft CSD codes predict reasonably well the variation of M^2C_n at r/R = 0.75, 0.87, and 0.97 in terms of the waveform and the phase; however, both analyses moderately over-predict M^2C_n at r/R = 0.97 at around the azimuth angle of 180°. In addition, M^2C_n at r/R = 0.87 predicted by CAMRAD II shows a small up-down behavior due to a spurious BVI event at around the azimuth angle of 0°. This CAMRAD II result seems contrary to both the measured data and DYMORE II prediction. This is because the present multiple-trailer wake model with consolidation in CAMRAD II analysis does not represent exactly the rotor wakes in BVI.

The correlation studies of M^2C_n for the MN case are given in Fig. 3. Compared with the BL case, the three-per-rev M^2C_n

variations in both the measured data and the predictions become stronger since the three-per-rev HHC inputs given in Table 2 are applied for this MN case. It is noticeable that the number of measured BVI events on the advancing side is reduced significantly. The overall trend of correlation between the predictions and the test data is reasonably good, although CAMRAD II and DYMORE II both show spurious BVI events in the first quadrant at all the three blade span locations. These spurious BVI events are caused from that the present analyses using the freewake models do not predict accurately the miss-distance defined as the vertical distance between a blade and the trailed vortices which is one of the driving factors affecting the rotor BVI noise. DYMORE II predicts the peak-to-peak magnitude of M^2C_n well than CAMRAD II; however, it moderately over-predicts the fluctuation magnitude of M^2C_n on the first quadrant. In addition, DYMORE II analysis predicts well the negative loading of M^2C_n at r/R = 0.97, but CAMRAD II prediction does not show it clearly.

Fig. 4 shows the measured and predicted section normal forces for the MV case. As in the previous MN case, the measured and predicted M^2C_n for the MV case both show more distinct three-per-rev M^2C_n variation than the BL case. The negative loadings of M^2C_n are definitely observed in the measured data at r/R = 0.87 and 0.97. CAMRAD II and DYMORE II both moderately or significantly under-predict the peak-to-peak magnitude of M^2C_n at all the three blade span locations and do not predict the negative loadings of M^2C_n at r/R = 0.87 and 0.97. However the fluctuations of M^2C_n predicted by CAMRAD II and DYMORE II are similar to each other; in addition they are compared reasonably well with the measured data on both advancing and retreating sides. Furthermore, as in the previous BL case, the M^2C_n at r/R = 0.87 in CAMRAD II analysis shows a quite small up and down behavior at around the azimuth angle of 0° which is due to a spurious BVI event prediction. Also, CAMRAD II over-predicts considerably the fluctuation magnitude of M^2C_n at r/R = 0.97 in the first quadrant. These are caused from that the present wake model does not describe accurately the BVI phenomenon, as previously discussed.

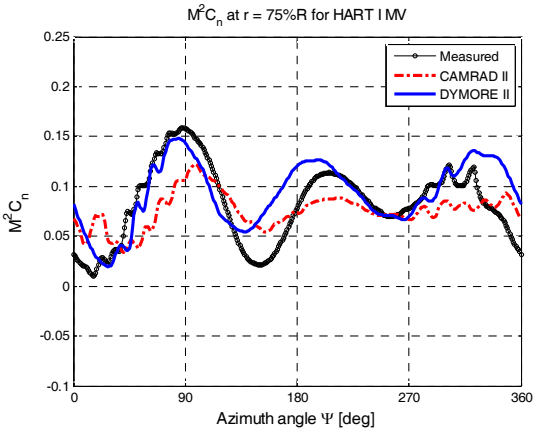

(a) r/R = 0.75

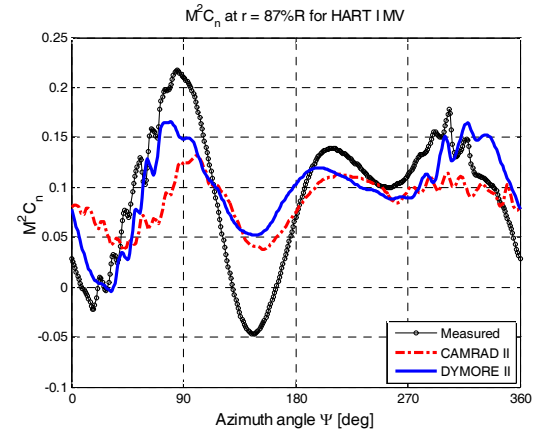

(b) r/R = 0.87

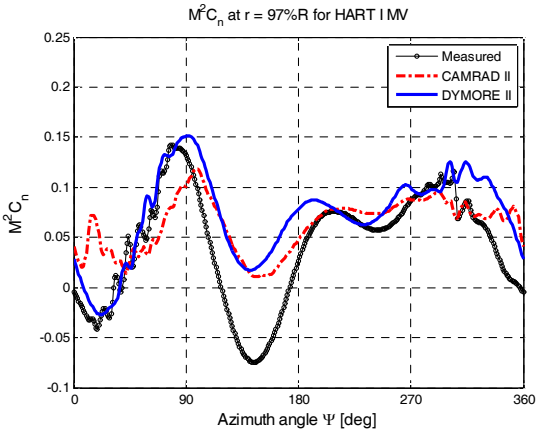

(c) r/R = 0.97

Fig. 4. Correlations of the section normal force (M^2C_n) for the MV case.

4.3 Rotor trim

The collective, lateral and longitudinal cyclic pitch control angles are adjusted by the rotorcraft CSD codes (CAMRAD II and DYMORE II) to match the measured thrust, hub rolling and pitching moments of which values are given in Ref. [1]. Fig. 5 shows the correlations of the trimmed pitch control angles in the present predictions and the measured data for the BL, MN, and MV cases. As seen in the figures, CAMRAD II and DYMORE II both over-predict the trimmed collective pitch angle θ_0 in all the three test cases. However, in all the three test cases, the lateral cyclic pitch angle θ_{1c} is under-predicted, and the longitudinal cyclic pitch angle θ_{1s} is reasonably predicted. The under-prediction of θ_{1c} can be improved by the inclusion of a fuselage model [11]. The two prediction results are quite similar to each other; however, the predicted trimmed pitch control angles should be discussed along with the blade elastic torsion deformation which will be discussed in the next section.

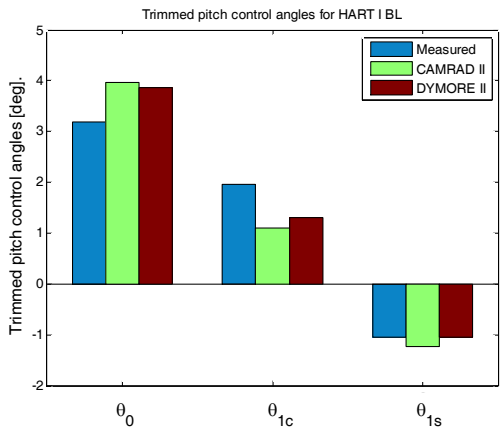

(a) BL

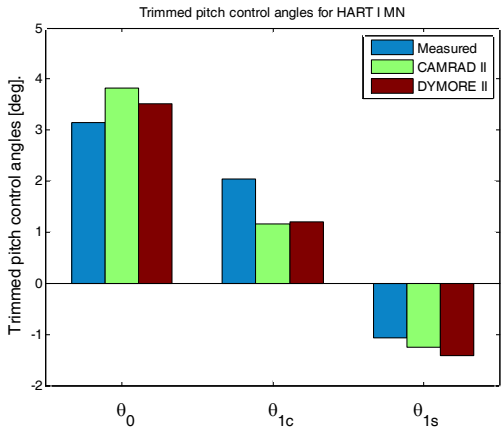

(b) MN

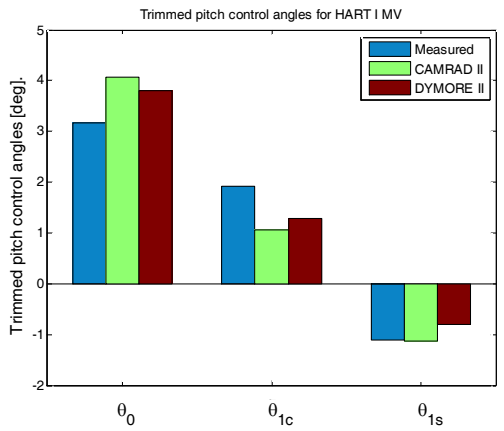

(c) MV

Fig. 5. Correlations of the trimmed pitch control angles.

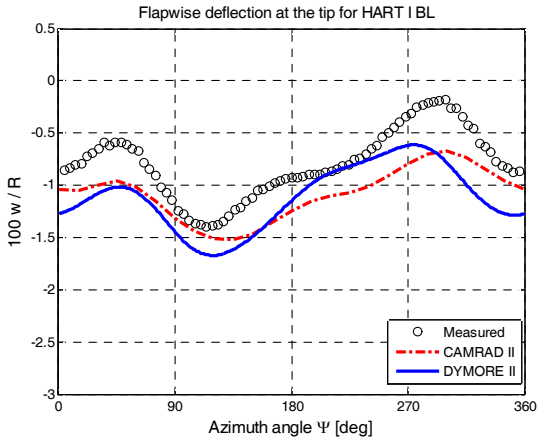

(a) BL

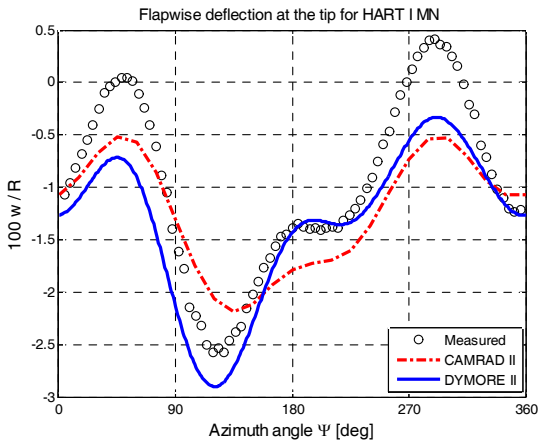

(b) MN

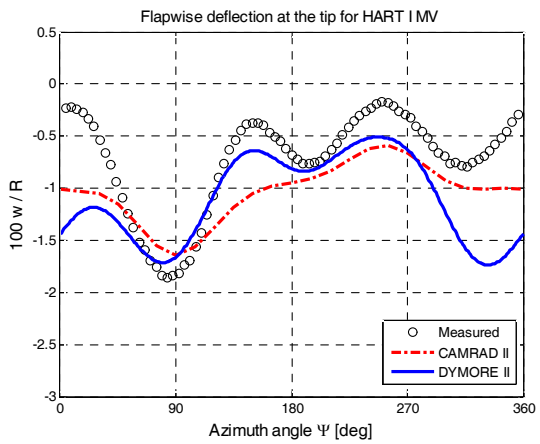

(c) MV

Fig. 6. Correlations of the flap deflection at the blade tip.

4.4 Blade elastic deformations

Figs. 6 and 7 correlate the predictions of the blade flap deflections (w) and elastic torsion deformations (ϕ) at the tip for the BL, MN, and MV cases with the measured data. The lead-lag deflection correlation is not conducted in this work since all the previous correlation studies for both HART I and II have shown a significant offset from the measured data. The flap deflection was measured without a precone angle, and its positive direction is defined as a flap-up. The elastic torsion deformation is defined without pitch controls and a pretwist, and the positive direction is defined as a nose-up.

Fig. 6 shows the correlation of the flap deflection at the blade tip in the BL, MN, and MV cases. For the BL case,

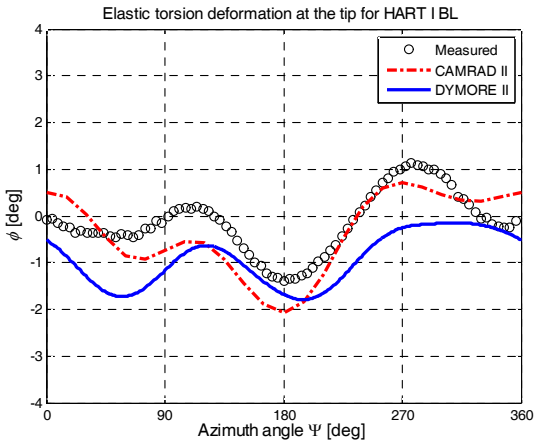

(a) BL

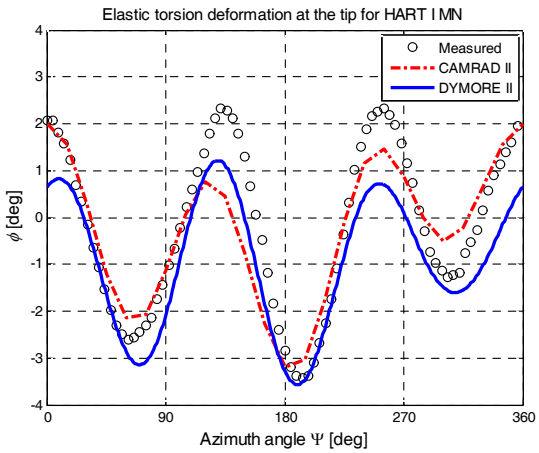

(b) MN

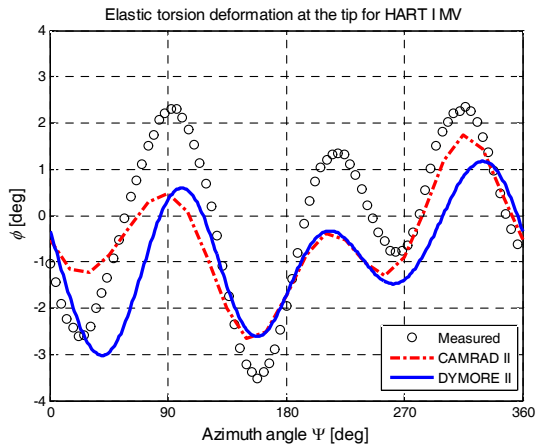

(c) MV

Fig. 7. Correlations of the elastic torsion deformation at the blade tip.

CAMRAD II and DYMORE II both correlate the measured data well. Although the mean values of the two prediction results both are moderately under-predicted, the peak-to-peak magnitudes and variations are fairly well predicted. For the MN case, as in the previous BL case, the results by CAMRAD II and DYMORE II both are compared well with the measured data in terms of the waveform and the phase. Furthermore, the two predictions are similar to each other. However, CAMRAD II and DYMORE II both under-predict the peak-to-peak magnitude since the present predictions use the section properties of the uninstrumented blade which is lighter than the reference blade with the measurement instruments [18]. For the MV case, the prediction results by CAMRAD II and DYMORE II both are not compared well with the measured data, unlike the previous BL and MN cases. The waveform predicted by CAMRAD II in the second and third quadrants is slightly different from the measured one. Although DYMORE II correlates well the waveform in the second and third quadrants with the test data, it significantly under-predicts the flap deflection at the blade tip in the aft of the rotor disk. Therefore, the comparison between the two analyses is also not as good as the results in the previous BL and MN cases.

The correlations of the elastic torsion deformation at the blade tip are given in Fig. 7. For the BL case, CAMRAD II and DYMORE II both capture the waveform well as compared with the measured data; however the prediction by CAMRAD II is better than the DYMORE II result since the peak-to-peak value and the phase by CAMRAD II are correlated better with the measured data than the correlation using DYMORE II. The mean values of the two rotorcraft CSD analyses are under-predicted as compared to the measured value. This is because the over-predicted collective pitch angle investigated in the previous section should be compensated with the steady elastic torsion deformation. For the MN case, the measured data and the rotorcraft CSD analyses both show the three-per-rev variation definitely. The predictions by CAMRAD II and DYMORE II both are correlated nicely with the measured data in terms of the waveform and the phase although the peak-to-peak magnitude is slightly under-predicted. In addition, the two predictions results are also quite similar to each other. For the MV case, as in the previous MN case, the wind tunnel test data and the two predictions both clearly exhibit the three-per-rev variation. The correlation between the predictions and the measured data is reasonably good; however, the peak-to-peak values by CAMRAD II and DYMORE II both are moderately under-predicted. The comparison between CAMRAD II and DYMORE II is good except that the down-up behavior in the first quadrant in the CAMRAD II analysis is moderately under-predicted.

4.5 Blade structural loads

Figs. 8-10 correlate the predicted blade structural loads such as the flap bending, lead-lag bending and torsion moments with the measured data for the BL, MN, and MV cases. The flap bending moment at r/R = 0.45, lead-lag bending moment at r/R = 0.51, and torsion moment at r/R = 0.40 are considered for the correlation. The positive directions of the flap bending, lead-lag bending, and torsion moments are defined as a bent-

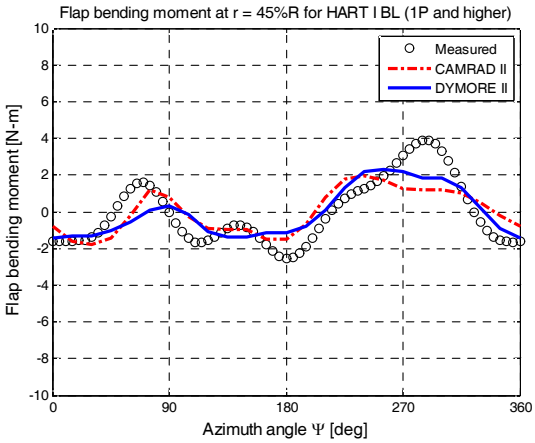

(a) BL

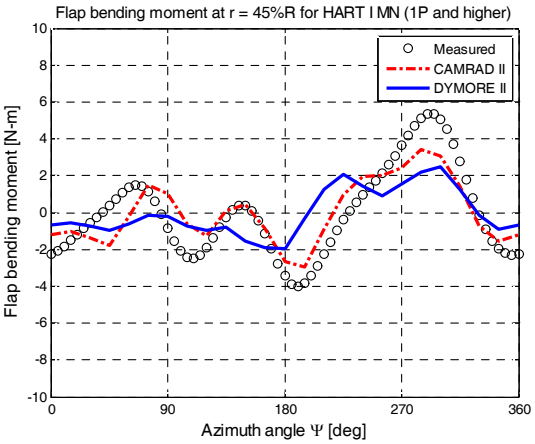

(b) MN

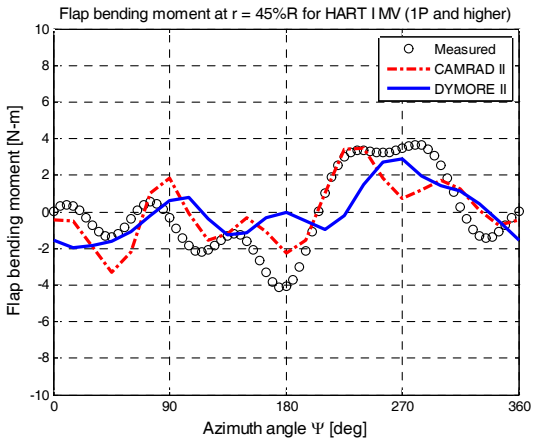

(c) MV

Fig. 8. Correlations of the oscillatory flap bending moment at r/R = 0.45.

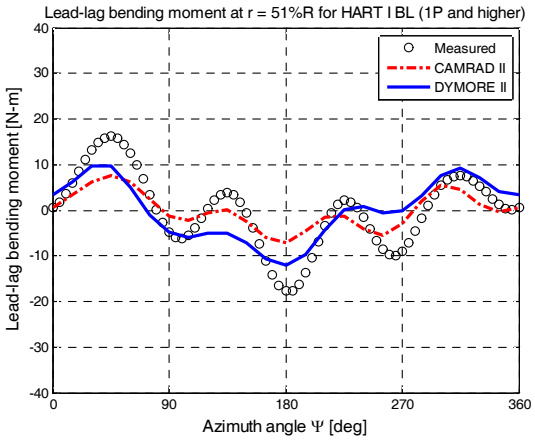

(a) BL

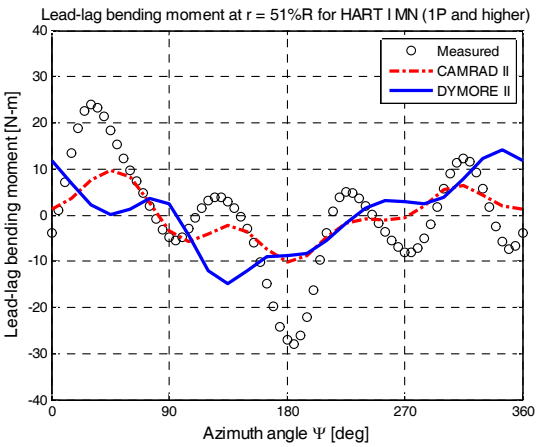

(b) MN

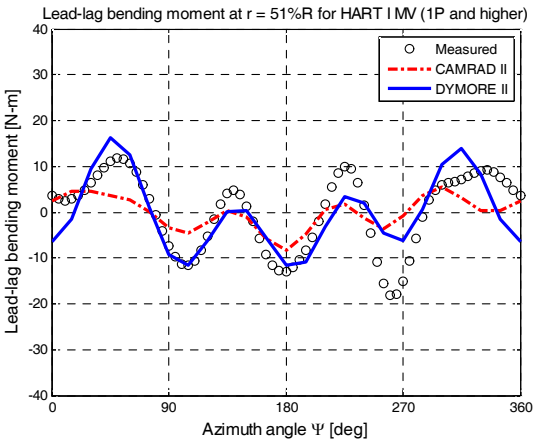

(c) MV

Fig. 9. Correlations of the oscillatory lead-lag bending moment at r/R = 0.51.

up, bent-forward (toward the leading edge), and pitch-up, respectively. Since a large offset in the mean values of the blade structural loads is usually observed between the prediction and measurement, the oscillatory loads without the mean values (1-per-rev and higher harmonics) are considered in the present correlation.

Fig. 8 correlates the predicted flap bending moments for the BL, MN, and MV cases with the measured data. For the BL case, the two analysis results by CAMRAD II and DYMORE II are quite similar to each other; in addition the correlation between the predictions and the measured data are also reasonable. However the predicted waveforms both are flattened

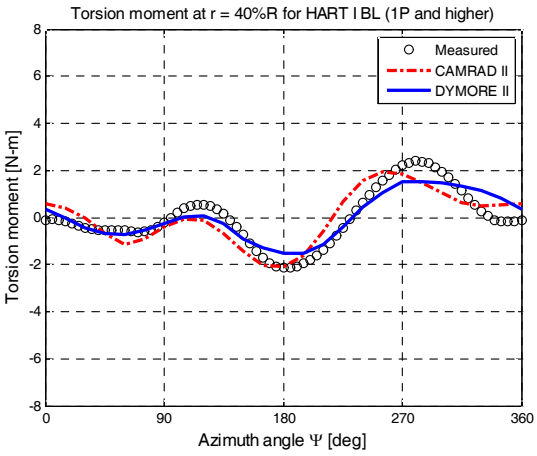

(a) BL

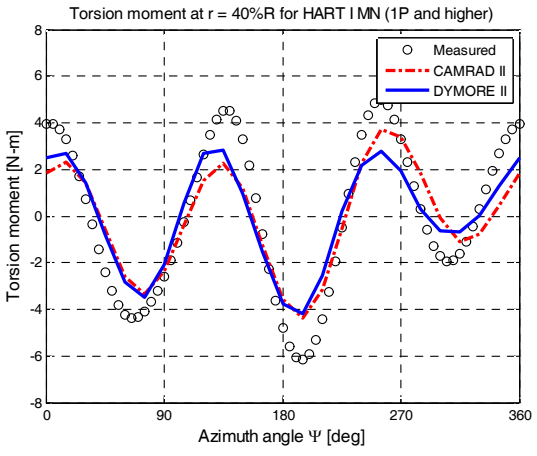

(b) MN

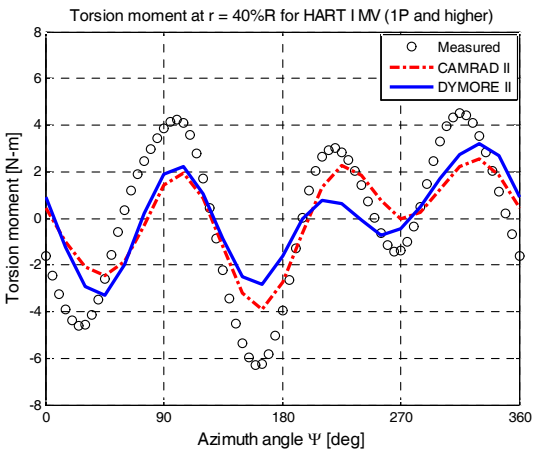

(c) MV

Fig. 10. Correlations of the oscillatory torsion moment at r/R = 0.40.

in the second and third quadrants. For the MN case, the CAMRAD II prediction correlates nicely with the measured data; however, DYMORE II analysis does not predict the waveform in the first and second quadrants well, although it captures the variation in the third and fourth quadrants fairly.

For the MV case, as in the previous MN case, the correlation using CAMRAD II is better than that with DYMORE II since DYMORE II does not capture well the behavior at around the azimuth angle of 180°. However, the comparison between CAMRAD II and DYMORE II is not poor in terms of the overall variation.

Fig. 9 gives the correlations of the lead-lag bending moments for the BL, MN, and MV cases. For the BL case, CAMRAD II and DYMORE II predictions both are correlated well with the measured data in terms of the waveform and the phase, although their peak-to-peak values are under-predicted. The two analysis results are also matched well to each other. For the MN case, CAMRAD II predicts reasonably the waveform and the phase although its peak-to-peak value is significantly under-predicted. The correlation between DYMORE II analysis and the measured data is poor. Therefore, DYMORE II prediction is not also matched well to the CAMRAD II result. For the MV case, unlike the previous MN case, the correlation of DYMORE II prediction with the measured data is slightly better than the comparison between CAMRAD II and the measured data since the variation and the peak-to-peak value both are predicted well by DYMORE II analysis. But, CAMRAD II result is also reasonably good as compared to the measured data.

The correlations of the torsion moments for the three test cases are shown in Fig. 10. For the BL case, the two rotorcraft CSD analysis results both are correlated nicely with the measured data and are quite similar to each other. For both the MN and MV cases, CAMRAD II and DYMORE II both correlate the waveform and the phase with the measured ones reasonably well; however, the peak-to-peak values in both the MN and MV cases are under-predicted. Furthermore, the two rotorcraft CSD predictions are matched well to each other.

5. Conclusions

In this work, the code-to-code comparison study using the two different rotorcraft CSD codes was conducted for the HART I with and without HHC inputs. As the rotorcraft CSD codes, CAMRAD II and DYMORE II were used. The predictions by CAMRAD II and DYMORE II were compared to each other and also correlated with the wind tunnel test data. The natural frequencies of a rotating blade, blade section normal forces, trimmed pitch control angles, blade elastic deformations at the tip, and blade structural loads were studied for the HART I BL, MN, and MV cases. From the present study, the following conclusions were obtained:

(1) Although CAMRAD II and DYMORE II used different modeling techniques for the HART I rotor system, the characteristics of rotating natural frequencies in the fan plot analysis were quite similar to each other. Furthermore, the predicted natural frequencies at non-rotating condition were matched reasonably well with the measured data. Therefore, it was considered that the structural dynamics characteristics using the two different rotorcraft CSD codes are close to each other

for the HART I rotor system.

(2) CAMRAD II and DYMORE II both correlated fairly well the blade section normal forces (M^2C_n) for the BL and MN cases with the measured data. Although some of the fluctuations were not predicted or spurious BVI events were observed, the fluctuations, the waveform, and the phase were reasonably predicted. However, the two rotorcraft CSD analyses for the MV case were not as good as the results in the BL and MN cases since the peak-to-peak values predicted by CAMRAD II and DYMORE II were significantly under-predicted and the negative loadings at r/R = 0.87 and 0.97 were not captured by both predictions.

(3) CAMRAD II and DYMORE II both over-predicted the trimmed collective pitch angle in the three test cases of HART I; however, this was compensated with the under-predicted mean value of the blade elastic torsion deformation. The comparison between CAMRAD II and DYMORE II results was good for the trimmed pitch control angles in the BL, MN, and MV cases.

(4) All the predicted results on blade elastic deformations at the tip showed reasonable correlations with the measured data except the flap deflection for the MV case. CAMRAD II and DYMORE II both predicted the elastic torsion deformation at the blade tip well for the three test cases; however, the CAMRAD II result was slightly better than the DYMORE II prediction particularly for the BL case.

(5) CAMRAD II and DYMORE II both fairly predicted the blade structural loads, such as the flap bending, lead-lag bending, and torsion moments. However, CAMRAD II showed moderately better correlation with the measured data than the DYMORE II prediction.

(6) Through the code-to-code comparison study using CAMRAD II and DYMORE II for the HART I aeromechanics, the prediction results by the two comprehensive analyses on the BVI airloads, rotor trim, blade elastic deformations, and blade structural loads were reasonably similar to each other. However, the CAMRAD II analysis using the multiple-trailer wake model with consolidation showed better correlation with the measured data, particularly for the blade structural loads prediction, than the DYMORE II prediction with the single wake panel model.

(7) Although the present analyses using the two different freewake models both showed reasonably good correlations on the rotor aeromechanics with the wind tunnel test data; however there were some prediction inaccuracies such as the prediction of the spurious BVI events, the under-prediction of peak-to-peak value of M^2C_n for the MV case and the over-prediction of the collective pitch control angle for all the test cases. This inaccuracy of the prediction is mainly due to the low fidelity aerodynamics model based on the lifting line theory with the freewake model used for the present study. Particularly the rotor aeromechanics analysis using a freewake model depends on seriously the empirical parameters for the freewake modeling. These theoretical limitations and drawbacks will be solved through the rotorcraft CSD/CFD coupled analysis.

Acknowledgment

This work was supported by research fund of Chungnam National University. The authors thank the HART I team for the test data.

Nomenclature

c	: Blade chord length, m
C_T	: Rotor thrust coefficient
C_n	: Section normal force coefficient
M	: Local Mach number
r	: Blade radial station, m
R	: Blade radius, m
θ_{3P}	: 3-per-rev pitch control magnitude, degrees
σ	: Rotor solidity
ψ	: Rotor azimuth angle, degrees
ψ_{3P}	: 3-per-rev pitch control phase, degrees

References

[1] W. R. Splettstoesser, R. Kube, U. Seelhorst, W. Wagner, A. Boutier, F. Micheli, E. Mercker and K. Pengel, Higher harmonic control aeroacoustic rotor test (HART) - Test document and representative results, *Institute Report IB 129-95/28*, German Aerospace Center (DLR), Braunschweig, Germany (1995).

[2] Y. H. Yu, C. Tung, B. G. van der Wall, H.-J. Pausder, C. Burley, T. Brooks, P. Beaumier, Y. Delrieux, E. Mercker and K. Pengel, The HART-II test : rotor wakes aeroacoustics with Higher-Harmonic pitch Control (HHC) inputs -The joint German/French/Dutch/US project-, *Proceedings of the American Helicopter Society 58th Annual Forum*, Montreal, Canada (2002).

[3] B. G. van der Wall, 2nd HHC Aeroacoustic Rotor Test (HART II) - Part II: Representation results-, *Institute Report IB 111-2005/03*, German Aerospace Center (DLR), Braunschweig, Germany (2005).

[4] J. W. Lim and B. G. van der Wall, Investigation of the effect of a multiple trailer wake model for descending flights, *Proceedings of the American Helicopter Society 61st Annual Forum*, Grapevine, Texas, USA (2005).

[5] J.-S. Park and S. N. Jung, Comprehensive multibody dynamics analysis for rotor aeromechanics predictions in descending flight, *The Aeronautical Journal*, 116 (1177) (2012) 229-249.

[6] B. G. van der Wall, J. W. Lim, M. J. Smith, S. N. Jung, J. Bailly, J. D. Baeder and D. D. Boyd Jr., An assessment of comprehensive code prediction state-of-the-art using the HART II international workshop data, *Proceedings of the American Helicopter Society 68th Annual Forum*, Ft. Worth, TX., USA (2012).

[7] H.-Y. Ryu and S.-J. Shin, Prediction of the aeromechanics for HART II rotor in descending flight using mixed variational geometrically exact beam analysis, *Journal of Me-*

chanical Science and Technology, 29 (1) (2015) 141-150.
[8] C.-M. Yang, Y. Inada and T. Aoyama, BVI noise prediction using motion data, *Proceedings of the 1st International Forum on Rotorcraft Multidisciplinary Technology*, Seoul, Korea (2007).
[9] J.-H. Sa, J.-W. Kim, S.-H. Park, J. -S. Park, S. N. Jung and Y. H. Yu, KFLOW results of airloads on HART-II rotor blades with prescribed blade deformation, *Proceedings of the 2nd International Forum on Rotorcraft Multidisciplinary Technology*, Seoul, Korea (2009).
[10] M. J. Smith, J. W. Lim, B. G. van der Wall, J. D. Baeder, R. T. Biedron, D. D. Boyd Jr., B. Jayaraman, S. N. Jung and B.-Y. Min, An assessment of CFD/CSD prediction state-of-the-art using the HART II international workshop data, *Proceedings of the American Helicopter Society 68th Annual Forum*, Ft. Worth, TX, USA (2012).
[11] J.-S. Park, J.-H. Sa, S.-H. Park, Y.-H. You and S. N. Jung, Loosely coupled multibody dynamics-CFD analysis for a rotor in descending flight, *Aerospace Science and Technology*, 29 (1) (2013) 262-276.
[12] C. Tung, J. M. Gallman, R. Kube, W. Wagerm, B. G. van der Wall, T. Brooks, C. L. Burley, D. D. Boyd Jr., G. Rahier and P. Beaumier, Prediction and measurement of blade-vortex interaction loading, *Proceedings of the CEAS/AIAA Aeroacoustics Conference*, Muenchen, Germany (1995).
[13] P. Beaumier and R. Spiegel, Validation of ONERA aeroacoustic prediction methods for blade-vortex interaction using HART test results, *Proceedings of the American Helicopter Society 51st Annual Forum*, Ft. Worth, TX, USA (1995).
[14] T. Brooks, D. D. Boyd Jr., C. Burley and J. Jolly Jr., Aeroacoustics codes for rotor harmonics and BVI noise CAMRAD.Mod1/HIRES, *Proceedings of the 2nd CEAS/AIAA Aeroacoustics Conference*, State College, PA, USA (1996).
[15] J. W. Lim, Y. H. Yu and W. Johnson, Calculation of rotor blade-vortex interaction airloads using a multiple-trailer free-wake model, *Journal of Aircraft,* 40 (6) (2003) 1123-1130.
[16] H. S. Yeo and W. Johnson, Assessment of comprehensive analysis calculation of airloads on helicopter rotors, *Journal of Aircraft,* 42 (5) (2005) 1218-1228.
[17] H. S. Yeo and W. Johnson, Prediction of rotor structural loads with comprehensive analysis, *Journal of The American Helicopter Society,* 53 (2) (2008) 193-209.
[18] S. N. Jung, Y.-H. You, B. H. Lau, W. Johnson and J. W. Lim, Evaluation of rotor structural and aerodynamic loads using measured blade properties, *Proceedings of the 38th European Rotorcraft Forum*, Amsterdam, Netherlands (2012).
[19] W. Johnson, *CAMRAD II, comprehensive analytical model of rotorcraft aerodynamics and dynamics*, Johnson Aeronautics (1992).
[20] O. A. Bauchau, Computational schemes for flexible, nonlinear multi-body systems, *Multibody System Dynamics*, 2 (2) (1998) 169-225.
[21] D. H. Hodges, A mixed variational formulation based on exact intrinsic equations for dynamics of moving beams, *International Journal of Solids and Structures*, 26 (11) (1990) 1253-1273.
[22] D. A. Peters, S. Karunamoorthy and W.-M. Cao, Finite state induced flow models Part I: two-dimensional thin airfoil, *Journal of Aircraft,* 32 (2) (1995) 313-322.
[23] D. A. Peters and C. J. He, Finite state induced flow models part II: three-dimensional rotor disk, *Journal of Aircraft,* 32 (2) (1995) 323-333.
[24] M. J. Bhagwat and J. G. Leishman, Stability, consistency and convergence of time-marching free-vortex rotor wake algorithms, *Journal of the American Helicopter Society,* 46 (1) (2001) 59-71.
[25] H. B. Squire, The growth of a vortex in turbulent flow, *Aeronautical Quarterly,* 16 (1965) 302-306.
[26] D. A. Peters and D. Barwey, A general theory of rotorcraft trim, *Mathematical Problems in Engineering,* 2 (1) (1965) 1-34.

Jae-Sang Park received Ph.D. degree in mechanical and aerospace engineering from Seoul National University, Seoul, Korea in 2006. From 2006 to 2007, he worked as a post doctor at Flight Vehicle Research Center, Seoul National University. From 2008 to 2013, he worked for the International Rotorcraft R&D Hub at Konkuk University, Seoul, Korea. Dr. Park is currently an assistant professor, Department of aerospace engineering, Chungnam National University, Daejeon, Korea. His research interests include aeroelasticity, rotorcraft aeromechanics and smart structures.

Young Jung Kee received his M.S. and Ph.D. degrees in mechanical and aerospace engineering from Seoul National University in 2003 and 2015, respectively. Since 2003, he has been a research engineer at the Rotorcraft Research team in Korea Aerospace Research Institute. His research interests include rotorcraft dynamics, static and fatigue tests of composite structures.